


Article

An Investigation on the Thermally Induced Compatibilization of SBR and α -Methylstyrene/Styrene Resin

Arnaud Wolf^{1,2}, João Paulo Cosas Fernandes¹ , Chuanyu Yan^{1,2}, Reiner Dieden¹ , Laurent Poorters³, Marc Weydert³ and Pierre Verge^{1,*} 

¹ Luxembourg Institute of Science and Technology, L-4362 Esch-sur-Alzette, Luxembourg; arnaud.wolf@list.lu (A.W.); joao.cosas@list.lu (J.P.C.F.); chuanyu.yan@list.lu (C.Y.); reiner.dieden@list.lu (R.D.)

² University of Luxembourg, L-4365 Esch-sur-Alzette, Luxembourg

³ Goodyear Innovation Center, L-7750 Colmar-Berg, Luxembourg; laurent_poorters@goodyear.com (L.P.); marc_weydert@goodyear.com (M.W.)

* Correspondence: pierre.verge@list.lu

Abstract: The miscibility between two polymers such as rubbers and performance resins is crucial to achieve given targeted properties in terms of tire performances. To this aim, α -methylstyrene/styrene resin (poly(α MSt-co-St)) are used to modify the viscoelastic behavior of rubbers and to fulfill the requirements of the final applications. The initial aim of this work was to understand the influence of poly(α MSt-co-St) resins blended at different concentrations in a commercial styrene-butadiene rubber (SBR). Interestingly, while studying the viscoelastic properties of SBR blends with poly(α MSt-co-St), crosslinking of the rubber was observed under conditions where it was not expected to happen. Surprisingly, after the crosslinking reactions, the poly(α MSt-co-St) resin was irreversibly miscible with SBR at concentrations far above its immiscibility threshold. A detailed investigation involving characterization technics including solid state nuclear magnetic resonance led to the conclusion that poly(α MSt-co-St) is depolymerizing under heating and can graft onto the chains of SBR. It results in an irreversible compatibilization mechanism between the rubber and the resin.

Keywords: compatibilization; rheology; atomic force microscopy; solid-state NMR



Citation: Wolf, A.; Fernandes, J.P.C.; Yan, C.; Dieden, R.; Poorters, L.; Weydert, M.; Verge, P. An Investigation on the Thermally Induced Compatibilization of SBR and α -Methylstyrene/Styrene Resin. *Polymers* **2021**, *13*, 1267. <https://doi.org/10.3390/polym13081267>

Academic Editor: Dariusz M. Bieliński

Received: 24 March 2021
Accepted: 9 April 2021
Published: 13 April 2021

Publisher's Note: MDPI stays neutral with regard to jurisdictional claims in published maps and institutional affiliations.



Copyright: © 2021 by the authors. Licensee MDPI, Basel, Switzerland. This article is an open access article distributed under the terms and conditions of the Creative Commons Attribution (CC BY) license (<https://creativecommons.org/licenses/by/4.0/>).

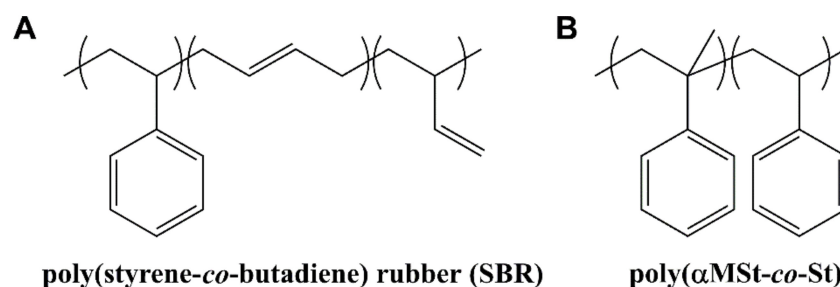
1. Introduction

The specifications of applicative materials are generally obtained by blending polymers of different chemical and physical characteristics [1–4]. Their miscibility is a crucial parameter to reach the targeted properties [5–7]. In the tire industry, rubbers are particularly subjected to an adjustment of their viscoelastic properties by their blending with another polymer [8–10]. Among them, poly(styrene-co-butadiene) rubber (SBR, Scheme 1A) is the main component of tire tread formulations thanks to its relatively high glass transition temperature (T_g) compared to other elastomers, as well as the temperature dependence of its loss factor [8,11]. Nevertheless, a modification of its viscoelastic properties is needed to fit the wet and dry grip requirements and to maximize its performance. Its blending with performance resins is a way to reach these specifications [12].

Performance resins regroup amorphous materials with a low average molecular weight (between 800 and 4000 g/mol). Three groups of synthetic performance resins can be found [13,14]: (i) Resins derived from naturally occurring terpenes produced from monomers isolated from pine trees, (ii) Coumarone-indene resins produced from monomers obtained by distillation of coal tar, and (iii) Aliphatic C₅ and aromatic C₉ hydrocarbon resins produced from monomers obtained via steam cracking of petroleum streams. These resins are widely used due to their efficiency to modify the viscoelastic behavior of rubbers to fulfil the requirements of the final applications [15–22].

Copolymers of α -methylstyrene and styrene (poly(α MSt-co-St)) belong to the group of aromatic C₉ hydrocarbon resins (Scheme 1B) [13]. In spite of the extensive use of these

resins, the literature is not rich in studies describing the resin concentration influence on the viscoelastic behavior of their blend with a rubber. The initial aim of this work was to fill this gap by assessing the viscoelastic properties of SBR and poly(α MSt-*co*-St) blends at different resin concentrations, from 25 to 150 parts per hundred rubber (phr). As the thermodynamic properties of polymer blends is highly dependent on the molecular weight [4,23–25], tailor-made and well-defined poly(α MSt-*co*-St) resins were prepared to avoid any side-effects from the molecular dispersity of the resin [26].



Scheme 1. Chemical structure of (A) poly(styrene-*co*-butadiene) rubber (SBR) and (B) poly(α MSt-*co*-St) resin.

Commercial SBR formulations are known to be mixed with an antioxidant system to prevent their thermal degradation and self-crosslinking [9]. Interestingly, while studying the viscoelastic properties of SBR blends with poly(α MSt-*co*-St), crosslinking of the rubber was observed under conditions where it was not expected to happen. When a polymer crosslinks while dissolved in a second polymer, it leads to a phase separation. This phenomenon, called reaction-induced phase separation (RIPS), results in a narrowing of the miscible concentration range, together with the increase of the polymerization or crosslinking density [27–34]. Surprisingly, after the crosslinking reactions, the poly(α MSt-*co*-St) resin was miscible with SBR at concentrations far above the immiscibility threshold.

This work reports on the investigation of this behavior and attempts to provide an explanation.

2. Materials and Methods

2.1. Materials

For the resin synthesis, Styrene $\geq 99\%$ (St, Sigma Aldrich) and α -methylstyrene $\geq 99\%$ (α MSt, Sigma Aldrich BVBA, Diegem, Belgium) were distilled over calcium hydride (CaH_2) under reduced pressure (~ 30 mbar) prior to reaction. Tetrahydrofuran (THF), cyclohexane and toluene (SLR grade, ThermoFisher Acros BVBA, Geel, Belgium) were purified through an MBraun SPS solvent purification system (alumina and 4 Å sieves columns). The solvent drums were degassed with flowing nitrogen (Alphagaz 2, Air Liquide, Rodange, Luxembourg) at least 30 min prior to the reaction. THF was distilled over sodium/benzophenone ($\text{Na}(0)$, $\geq 99.8\%$ oiled sticks in aluminum foil, and benzophenone, 99% ReagentPlus[®], Sigma Aldrich BVBA, Diegem, Belgium) by refluxing while a purple color was observed. Methanol (MeOH , $\geq 99.8\%$ ExtraDry over molecular sieves, stored under argon, Acros organics BVBA, Geel, Belgium) and *n*-BuLi (2.5 M in hexane, stored under argon at 4 °C, Acros Organics BVBA, Geel, Belgium) were used as received.

For the resin/rubber blend preparation, styrene-butadiene rubber (SBR, Sprintan SLR4602, Trinseo BVBA, Luxembourg, Luxembourg) was used as received. Tetrahydrofuran (THF, SLR grade, ThermoFisher Acros BVBA, Geel, Belgium) was purified through an MBraun SPS solvent purification system (alumina and 4 Å sieves columns). Dicumyl peroxide (DCP, 98%, Sigma Aldrich BVBA, Diegem, Belgium) was purified by recrystallization from MeOH prior use. Hydroquinone (ReagentPlus[®] $\geq 99\%$, Sigma Aldrich BVBA, Diegem, Belgium) was used as received.

For the swelling test, toluene (SLR grade, ThermoFisher Acros BVBA, Geel, Belgium) was passed through an MBraun SPS solvent purification system (alumina and 4 Å sieves columns) prior to use.

2.2. Synthesis of Poly(α MSt-co-St) Resin

Poly(α MSt-co-St) resin with a molecular weight of 1820 g/mol was prepared via anionic copolymerization using the equimolar aliquot addition method, following a procedure reported previously [26]. Molecular characteristics are described in the Supplementary Materials (Section S1).

2.3. SBR/Poly(α MSt-co-St) Blending Procedure

Poly(α MSt-co-St) resin was mixed with SBR rubber via solution mixing. A summary of the blend's composition is described in the Supplementary Materials (Section S2, Table S1). The preparation of SBR/poly(α MSt-co-St)₁₅₀ is given as an example. Approximately, 0.12 g of synthesized poly(α MSt-co-St) and 0.08 g of SBR (60:40 mixture, 150 phr) were weighed and dissolved in 5 mL of THF until complete homogenization. For rheological measurements, the solution was casted onto a poly(tetrafluoroethylene) (PTFE)-covered glass Petri dish and dried overnight under the hood at room temperature. This treatment was sufficient to remove the traces of solvent. A rubber film was thus recovered and compressed into a rubber ball.

2.4. Rheological Measurements

The rheometer used was an MCR302 equipped with a heating chamber CTD450L (Anton Paar, Graz, Austria). The lower plate was a disposable PP25 and the upper plate was a PP8 (SN50810) measuring system from Anton Paar. The blend was first loaded at 25 °C under the parallel plates and squeezed to have a gap of 1 ± 0.3 mm. The blend was then trimmed to avoid any side effects during the measurements. For the rheological measurements of SBR/poly(α MSt-co-St) blends at different resin concentrations, the sample was first heated up to 160 °C and stabilized during ~1 min, to remove any internal constraints due to the solvent casting method. The measurement started directly after the stabilization following a 5 °C/min cooling ramp until −50 °C. The applied shear during measurement was following a linear ramp from 1 to 0.02% from 160 to −10 °C. From −10 °C, the applied shear was set to 0.01% to avoid any ruptures due to the maximum torque limit of the instrument. To characterize SBR crosslinking and resin compatibilization by rheology, the SBR/poly(α MSt-co-St)₁₅₀ blend was heated up to 215 °C with a temperature ramp of 5 °C/min. The blend was then cooled down directly after reaching 215 °C following a 5 °C/min cooling ramp until −80 °C. The applied shear during measurement was following a linear ramp from 0.1 to 2% from 25 to 215 °C, and from 2 to 0.1% from 215 °C to −10 °C. From −10 °C, the applied shear was constantly set to 0.02%. Due to thermal expansion of the sample, a dynamic normal force of ± 0.25 N was applied to maintain contact with the sample in each case.

2.5. Gel Permeation Chromatography Measurements

Gel permeation chromatography was performed using an Agilent 1200 Series (Agilent, Diegem, Belgium) equipped with PLgel mixed-C and Mixed-D columns and with three separate detectors (light scattering, viscosimeter and refractive index RI detector). The samples were prepared according to following procedure. A solution of ± 3 mg/mL was prepared by dissolving the polymer in THF (HPLC grade, 99.9%, extra pure, anhydrous, stabilized with 2,6-di-*tert*-butyl-4-methylphenol (BHT)). After homogenization, the solution was filtered through an Agilent PTFE 0.2 μ m filter to remove any dust or solid impurities. The solution was recovered in a 2 mL glass vial and placed in an automatic sample holder.

Prior to measurement, refractive index (RI) and viscosimeter detectors were purged and zero-tuned. The flow rate was set up at 1 mL/min constantly. The measurement started after the injection of 100 μ L of prepared solution. The measurement was stopped

after the delayed viscosimeter peak (35 min) to avoid interferences with the next sample. The molecular weight distributions were calculated thanks to a poly(styrene) standard calibration (Agilent EasyVial polymer standard, Diegem, Belgium) going from 100 g/mol to 300,000 g/mol.

2.6. Atomic Force Microscopy Measurements

A solution of SBR and poly(α MSt-co-St) in toluene was cast on a magnetic stainless-steel disc. The resin concentration was defined at 150 phr of poly(α MSt-co-St). The blend was dried overnight under the hood at room temperature. A thin film on the metal disc surface was recovered.

Images of the topography and nanomechanical properties of the samples were acquired using the bimodal AM-FM mode of the MFP-3D Infinity AFM (Asylum Research, Santa-Barbara, CA, USA). Two different setups were used to characterize the morphological changes at different temperatures and the nanomechanical properties at room temperature.

For morphological changes at different temperatures, AC160TS-R3 Olympus cantilevers (Asylum Research, Santa-Barbara, CA, USA) were used, mounted in a high temperature cantilever holder (PEEK). Since the holder is not adapted for quantitative nanomechanical analyses, only qualitative stiffness contrast was obtained. In AM-FM mode, the shift in contact resonance frequency of the second mode allows for the acquisition of complementary stiffness contrast simultaneously with the topography. For measurements at high temperature, a modular heating stage PolyHeater (Oxford Instruments, Gometz-la-Ville, France) was used, designed for high temperature polymer studies from ambient to 400 °C in air. The temperature was varied between 25 °C, 160 °C and 215 °C. Samples were imaged at 25 °C and 160 °C but due to the high mobility of the material at 215 °C, images could not be acquired at this temperature. Area of $10 \times 10 \mu\text{m}^2$ were imaged with a resolution of 256×256 pixels at a scan rate of 3 Hz.

For quantitative measurements of the nanomechanical properties, AC160TS-R3 cantilevers were mounted on a dedicated AM-FM Probe Holder. Cantilever spring constants were measured as about 23 N/m using the GetReal™ Automated Probe Calibration feature and the first and second resonant frequencies were determined to be 240 kHz and 1.33 MHz, respectively. A relative calibration method was used to estimate the tip radius using a dedicated reference samples kit (Model: PFQNM-SMPKIT-12m, Bruker, Karlsruhe, Germany). The tip radius was adjusted to obtain the proper value of 2.7 GPa for the polystyrene reference, matching the deformation applied on the sample of interest. To ensure repulsive intermittent contact mode, the amplitude setpoint was chosen as $A_{\text{setpoint}}/A_0 \sim 0.5$ to 0.7 so that the phase is well fixed below 70°. The reported average and standard deviation values of modulus consider at least 4 and up to 6 images in each sample for representative results.

2.7. Nuclear Magnetic Resonance Measurements

The liquid- and solid-state nuclear magnetic resonance (NMR) spectra were measured on a Bruker Avance III HD 600 MHz (proton Larmor frequency) spectrometer (Bruker, Karlsruhe, Germany). All the chemical shifts were referenced to tetramethylsilane (TMS) by referencing the residual d-chloroform signal to 7.26 ppm (liquid state) or setting the adamantane methylene signal to 37.77 ppm (solid state). For liquid-state NMR, ~20 mg of neat SBR was dissolved in ~600 μL of deuterated toluene-d₈ (99.6%D, Sigma Aldrich BVBA, Diegem, Belgium) in a 5 mm NMR tube. ¹³C spectra with inverse gated ¹H decoupling were performed on solution samples with a repetition delay of 6 s and a total accumulation of 10,240 scans. Prior to the swollen solid-state NMR experiments, samples were swollen and washed at least 3 times in 100 ml of toluene. To obtain the solid-state ¹³C NMR spectra, ~7 mg of crosslinked SBR (either with the resin CrR-SBR or with dicumyl peroxide CrDCP-SBR) was swollen by ~24 mg of toluene-d₈ in a disposable HRMAS insert (B4493, Bruker), which was inserted into a 4 mm ZrO₂ rotor and spun at 7 kHz spinning rate on a double-resonance MAS probe. One-dimensional ¹³C direct polarization with high-power

decoupling NMR experiments were performed on the CrR-SBR and CrDCP-SBR samples with a repetition delay of 4 s, and a total accumulation of 3288 and 2499 scans, respectively.

3. Results

3.1. Viscoelastic Characterization of SBR/Poly(α MSt-co-St) Blends at Different Resin Concentrations

The viscoelastic properties of SBR/poly(α MSt-co-St) blends at different resin concentrations ranging from 25 to 150 phr were determined by rheological measurements. The blends were first heated up to 160 °C, then cooled down to −50 °C. The storage modulus (G'), loss modulus (G'') and loss factor were determined during the cooling ramp. Figure 1 represents the viscoelastic properties of SBR/poly(α MSt-co-St) blends at concentrations from 25 to 60 phr (Figure 1A) and from 60 to 150 phr (Figure 1B) compared to neat SBR (black curves).

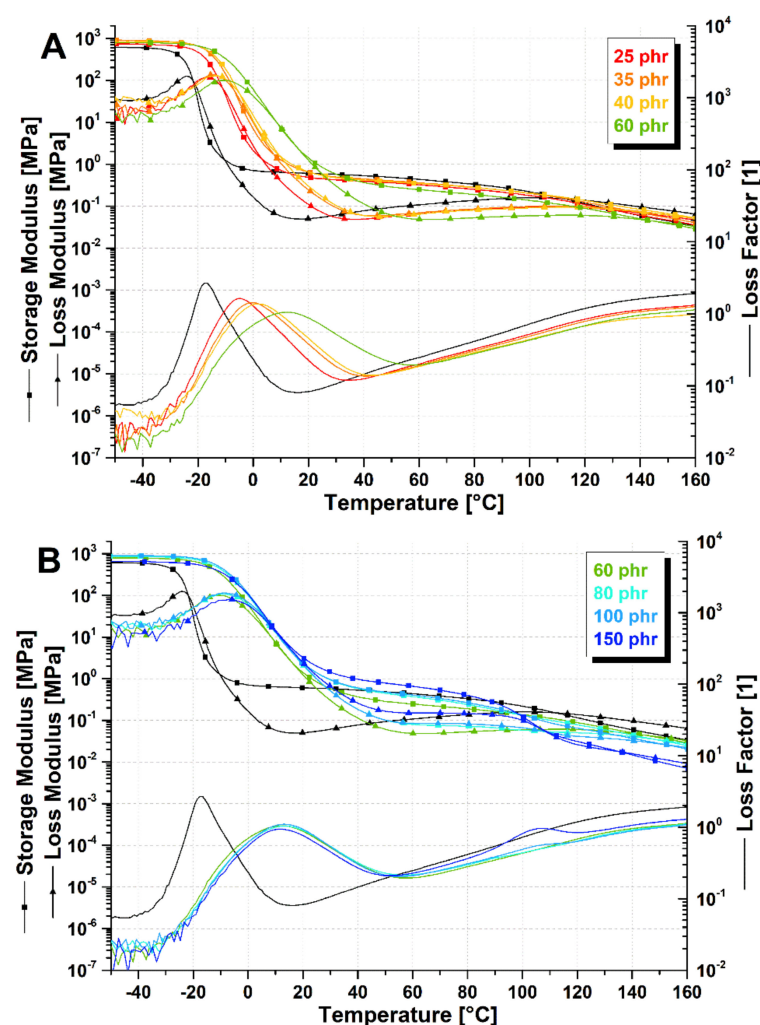


Figure 1. (A) Viscoelastic properties of styrene-butadiene rubber (SBR)/poly(α MSt-co-St) blends containing 25 to 60 phr of poly(α MSt-co-St) resin. (B) Viscoelastic properties of SBR/poly(α MSt-co-St) blends containing 60 to 150 phr of poly(α MSt-co-St) resin. Neat SBR is represented by the black curves. Properties measured during the cooling ramp (5 °C/min) from 160 °C to −50 °C.

The T_g of SBR was shifting depending on the resin concentration. Up to 60 phr, poly(α MSt-co-St) is fully miscible in SBR as only one T_g is detected. Between 60 and 80 phr, a second glass transition is starting to appear in the range of the resin T_g (around 80–120 °C), indicative of a phase separation. From 80 phr, the blend T_g is relatively constant and a clear biphasic behavior was observed. This value was taken as the immiscibility threshold of the

resin in SBR. The results suggest that SBR is saturated with poly(α MSt-co-St) resin, and the excess of resin is phase-separating.

3.2. Evidence of SBR/Poly(α MSt-co-St)₁₅₀ Blends Crosslinking and Enhanced Compatibility

SBR loaded with 150 phr of poly(α MSt-co-St) was selected to illustrate the SBR crosslinking and enhanced compatibility between both components, as an unambiguous phase separation was observed. When rheological measurements of SBR/poly(α MSt-co-St)₁₅₀ were performed while heating up from 20 to 215 °C, an increase of G' was observed. This trend was not expected since SBR alone did not show such behavior (Figure 2A, red curves). Surprisingly, the G' increase was the result of the crosslinking of SBR, as attested by swelling measurements of the tested samples immersed in toluene. Indeed, after the test, the sample swelled more than 2000% in toluene (Table 1). From the Flory-Rehner equation, the SBR crosslink density was calculated to be equal to 2.18×10^{-4} mol/cm³, corresponding to one crosslink node every 85,000 g/mol of SBR. It is noteworthy that SBR alone heated up to 215 °C remains fully soluble in toluene, as well as SBR/resin blends heated up to 160 °C. The crosslinking of SBR in the presence of the resin indicates that a thermally induced reaction occurred during the measurement.

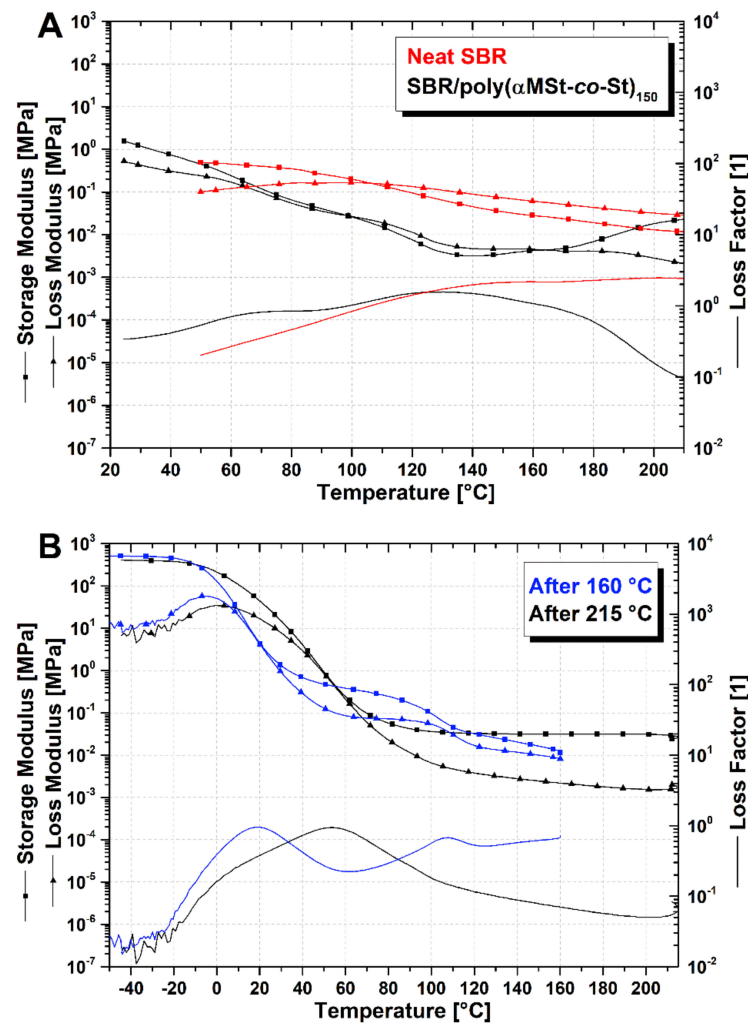


Figure 2. (A) Viscoelastic properties of neat SBR (red curves) and SBR/poly(α MSt-co-St)₁₅₀ blend (black curves) while heating up (5 °C/min) from 20 to 215 °C. (B) Comparison of SBR/poly(α MSt-co-St)₁₅₀ blend after heat treatment at 160 (blue curve) and 215 °C (black curve) during cooling ramp (5 °C/min) to −50 °C.

Table 1. Swelling test of SBR/poly(α MSt-co-St)₁₅₀ blend after rheological test at 215 °C.

Sample + Heat Treatment ¹	State	m Swell (g)	m Dry (g)	m Toluene (g)	%swelling	$V_e \times 10^4$ (mol/cm ³) ²
Neat SBR after 215 °C	Soluble	-	-	-	-	-
SBR/poly(α MSt-co-St) ₁₅₀ after 160 °C	Soluble	-	-	-	-	-
SBR/poly(α MSt-co-St) ₁₅₀ after 215 °C	Swollen	0.4062	0.0191	0.3871	2027	2.18

¹ heat treatment is defined as the maximum temperature the sample has been exposed to. ² Calculated with Flory–Rehner equation.

In addition, the measurement of the viscoelastic properties of SBR/poly(α MSt-co-St)₁₅₀ heated up to 215 °C exhibited a significantly different behavior than SBR/poly(α MSt-co-St)₁₅₀ heated only up to 160 °C. While the later revealed two glass transition temperatures indicating that the immiscibility threshold is passed (Figure 2B, blue curves), the blend heated up to 215 °C only had one relaxation (Figure 2B, black curves). This indicates that, after the thermal treatment at 215 °C, the miscibility of both components has been improved. The stability of this behavior was checked by successively re-measuring the sample three times with successful heating–cooling cycles between –50 and 160 °C (see Supplementary Materials, Section S3, Figure S1). In each case, just one single relaxation was observed, meaning this reaction was irreversible.

3.3. Atomic Force Microscopy Measurements of SBR/Poly(α MSt-co-St)₁₅₀

The phase behavior of SBR/poly(α MSt-co-St)₁₅₀ heated at either 160 °C or 215 °C was checked by following the evolution of the morphology by AFM. The control of the temperature was performed using a heating stage under the AFM head, for a duration of 20 min at each temperature.

Figure 3 shows images of SBR/poly(α MSt-co-St)₁₅₀ taken at 25 °C and sequentially heated at 160 °C at the same location. At 25 °C (Figure 3A), the stiffness contrast images of the area show homogeneous properties with no phase separation. It was assumed that the absence of phase-separation before the heat treatment was attributed to the solvent-casted blend preparation, which may induce a non-equilibrium state of mixing. At 160 °C, a clear phase separation is revealed in the stiffness contrast. Indeed, the softer SBR matrix appears in dark brown and the stiffer poly(α MSt-co-St) resin in light yellow. With a scan line of 3 Hz and 256 × 256 pixels, each image was taken in less than three minutes. In image B, one can see that the size of the phase-separated resin changes from a few hundred of nanometers in the beginning of the image (top) to a few microns at the end of the image (bottom), i.e., the phase separation and coalescence of the poly(α MSt-co-St) resin happened during imaging. The same effect can be seen in images C and D, until the system reaches stability, with the phase-separated resin reaching several microns in diameter. The bright, rough particle (probably dust on the surface) is an indication of the thermal drift of the sample under the tip. The last image F was taken with the dust particle as a reference of the location for imaging after treatment, which was retrieved after cooling, confirming that the phase-separation is retained (see Supplementary Materials, Section S4, Figure S2). The same experiment was repeated to confirm the trends observed. Complementary images (see Supplementary Materials, Section S4, Figure S3) consistently show the phase separation and coalescence of the poly(α MSt-co-St) resin, with sizes varying from ~200 nm to 3 μ m, which can be related to the local amount of resin at the imaged location, the thickness of the film and the duration of thermal treatment. These results agree with the rheological measurements performed at 160 °C which were showing the phase separation of poly(α MSt-co-St) at the same resin concentration (150 phr).

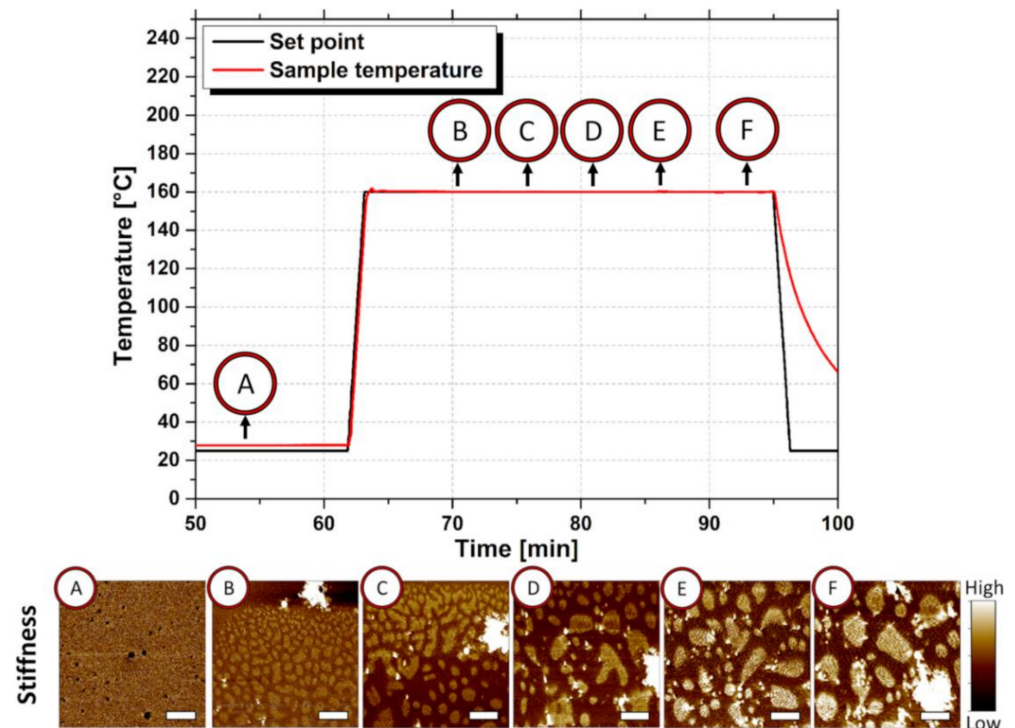


Figure 3. Temperature profile scheme and sequential stiffness contrast images of the SBR/poly(α MSt-co-St)₁₅₀ blend showing the phase separation and coalescence of poly(α MSt-co-St) domains. Images taken at (A) 25 °C and (B–F) 160 °C at various time. Scale bars on the images correspond to 2 μ m.

After proving the phase separation during heat treatment at 160 °C, a fresh sample (also at 150 phr resin loading) was thermally treated from 25 to 215 °C and images were taken at each step to follow the evolution of the morphology, as shown in Figure 4. The insets show representative images of the topography and stiffness contrast taken at each step. At 25 °C (Figure 4A), again no phase separation was seen in the stiffness contrast image. The sample was then heated at 200 °C/min up to 160 °C. The morphology observed on the images taken at 160 °C (Figure 4B) is similar to images recorded before on Figure 3. After slowly cooling back to 25 °C (Figure 4C), one can see by the stiffness contrast that the phase separation is maintained with the poly(α MSt-co-St) resin phase appearing as round domains of about 3 μ m in diameter. Phase separation is also seen in topography, which is rougher compared to the images recorded before the treatment, following the stiffness difference between the phases. Due to the low viscosity of the material at high temperature, it was impossible to acquire images at 215 °C. Nevertheless, images of the material at 25 °C after the treatment at 215 °C for 20 min (Figure 4D), show no phase separation, with a smooth surface and a homogeneous stiffness contrast, in excellent agreement with the rheological measurements done after the treatment of the samples at 215 °C.

Finally, quantitative nanomechanical measurements were done in the neat materials and on the blend at different steps of thermal treatment. Results are shown in Table 2. It is worth noting that elastomers being viscoelastic materials, their viscoelastic properties are time-dependent and therefore are greatly affected by the frequency of analysis. According to the Time–Temperature Superposition (TTS) principle [35,36], high frequency viscoelastic behavior is equivalent to lower temperatures, as the polymer chains do not have enough time to respond to the solicitation. The AM-FM modulus measurements are taken at \sim 1.3 MHz (second resonance frequency of the cantilever), therefore the values are higher than the usually reported for elastomeric materials at room temperature [37]. Nevertheless, the enhancement effect of the addition of the poly(α MSt-co-St) resin in the viscoelastic properties of SBR is verified. Furthermore, the properties are also affected by the thermal treatments, which might be related to the increasing miscibility of the resin in the SBR

matrix and crosslinking. Representative images and property histograms are shown in the Supplementary Materials (Section S4, Figure S4).

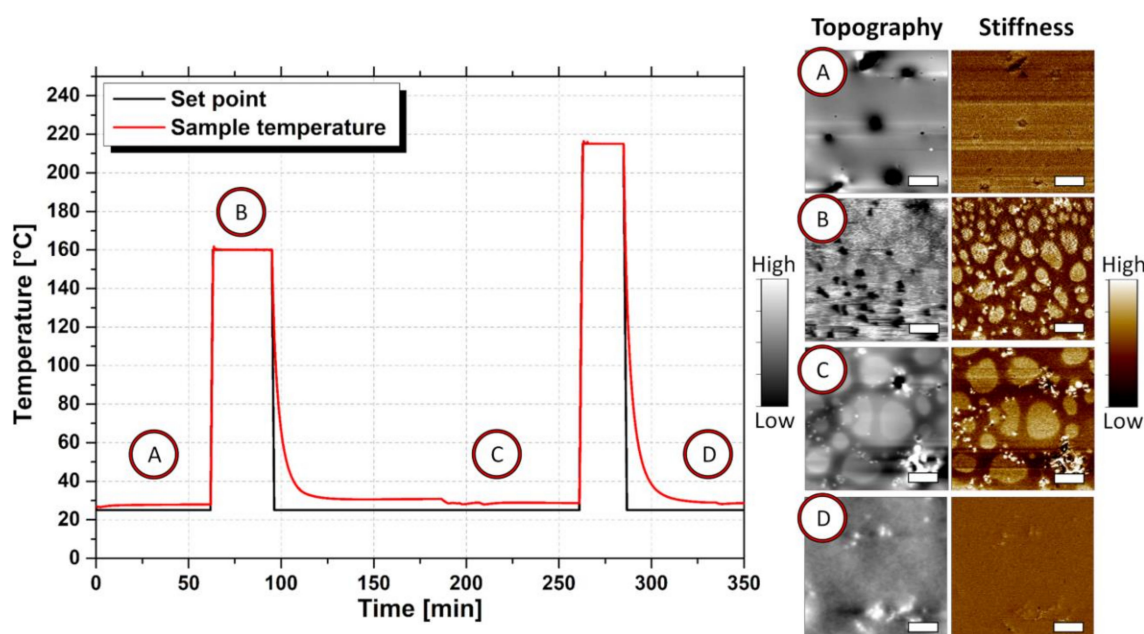


Figure 4. Temperature profile scheme and images of the topography and stiffness contrast of the SBR/poly(α MSt-co-St)₁₅₀ blend taken at each step. Images taken at (A) 25 °C, (B) 160 °C, (C) 25 °C after heat treatment at 160 °C and (D) 25 °C after the heat treatment at 215 °C. Scale bars on the images correspond to 2 μ m.

Table 2. Nanomechanical measurements of modulus in AM-FM.

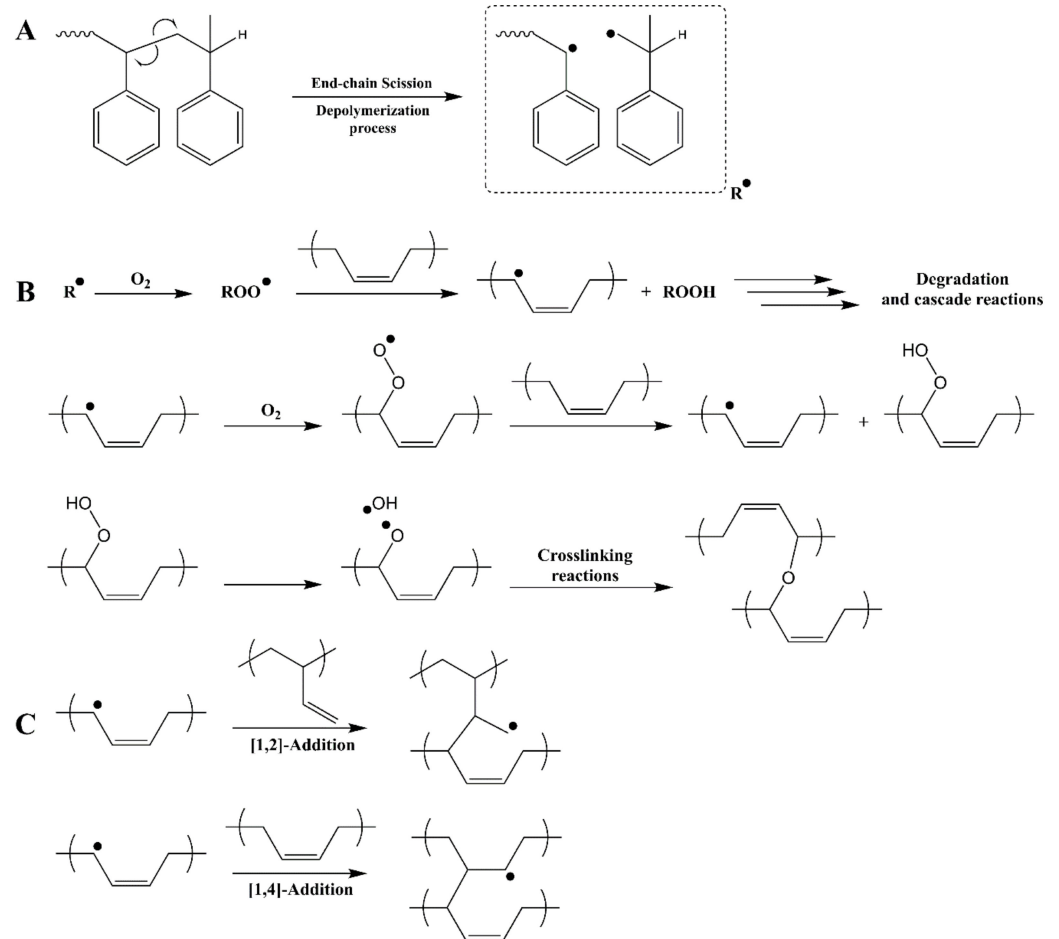
Sample + Heat Treatment	Modulus (GPa)		Morphology
	SBR	AMS	
Poly(α MSt-co-St)	-	3.6 \pm 0.4	Single phase
Neat SBR	0.80 \pm 0.05	-	Single phase
SBR/poly(α MSt-co-St) ₁₅₀	1.15 \pm 0.20	-	Single phase
SBR/poly(α MSt-co-St) ₁₅₀ after 160 °C	1.80 \pm 0.20	2.8 \pm 0.4	Dual phase
SBR/poly(α MSt-co-St) ₁₅₀ after 215 °C	2.00 \pm 0.35	-	Single phase

4. Discussion

The evolution of the viscoelastic properties of SBR with increasing resin concentration showed that poly(α MSt-co-St) possesses an immiscibility threshold around 80 phr. Above this concentration, SBR is saturated by the resin and the latter starts to phase-separate. Interestingly, after a heat treatment at 215 °C, SBR/poly(α MSt-co-St)₁₅₀ revealed miscibility far above its immiscibility threshold. Rheological measurements, swelling tests and AFM supported the conclusion that SBR was crosslinking in the presence of poly(α MSt-co-St) when heated up to 215 °C and lead to the resin compatibilization. This compatibilization was found to be stable over time.

These behaviors were not expected to happen. Indeed, it is known that antioxidants are added to commercial SBR formulations to prevent their thermal degradation and self-crosslinking [9]. It has been reported that when a polymer crosslinks while dissolved in a blend with a second polymer, it leads to a phase separation [27–34]. This phenomenon, called reaction-induced phase separation (RIPS), results in a narrowing of the miscible concentration range, together with the increase of the crosslinking density, due to the reduction of the entropy of mixing. Surprisingly, the opposite behavior was observed in the case of SBR/poly(α MSt-co-St)₁₅₀, suggesting another mechanism was occurring. The following discussion attempts to explain this behavior.

SBR alone is stable up to 225 °C (see Supplementary Materials, Section S5, Figure S5). However, poly(α MSt-*co*-St) resins are known to depolymerize under thermal conditions [38–40], leading to the formation of free-radicals by a mechanism of end-chain scission (Scheme 2A).



Scheme 2. (A) Thermal end-chain scission of poly(α MSt-*co*-St) resin. (B) Cascade of reactions leading to the oxidative crosslinking of SBR. (C) Representation of [1,2]- and [1,4]- addition crosslinking reactions. Scheme adapted from [41,42].

The alteration of the structural features of poly(α MSt-*co*-St) before and after a thermal heating of 24 h at 215 °C was shown by the determination of its molecular weight distribution (Figure 5). The gel permeation chromatography (GPC) traces depict a clear reduction of the resin molecular weight together with a significant increase of the dispersity (\bar{D}) due to the thermal treatment, in accordance with a radical scission and depolymerization of the resin. The generation of free radicals from the thermal depolymerization of poly(α MSt-*co*-St) (Scheme 2A) could be the origin of the crosslinking of the rubber during the rheological tests. Indeed, the radical crosslinking mechanism of SBR is a well-known phenomenon [38,41–45]. The free radicals generated by poly(α MSt-*co*-St) thermal depolymerization may initiate the oxidative crosslinking of the rubber (Scheme 2B). This step, also called “oxidative hardening” of the rubber, results in a cascade of crosslinking reactions involving oxygen. The radical on the α -position of the vinyl double bond is also highly reactive toward the unsaturation present in SBR and is able to successively react with the [1,2]- and the [1,4]-butadiene units, to form a crosslinked network, as a results of [1,2]- and [1,4]-addition crosslinking reactions (Scheme 2C).

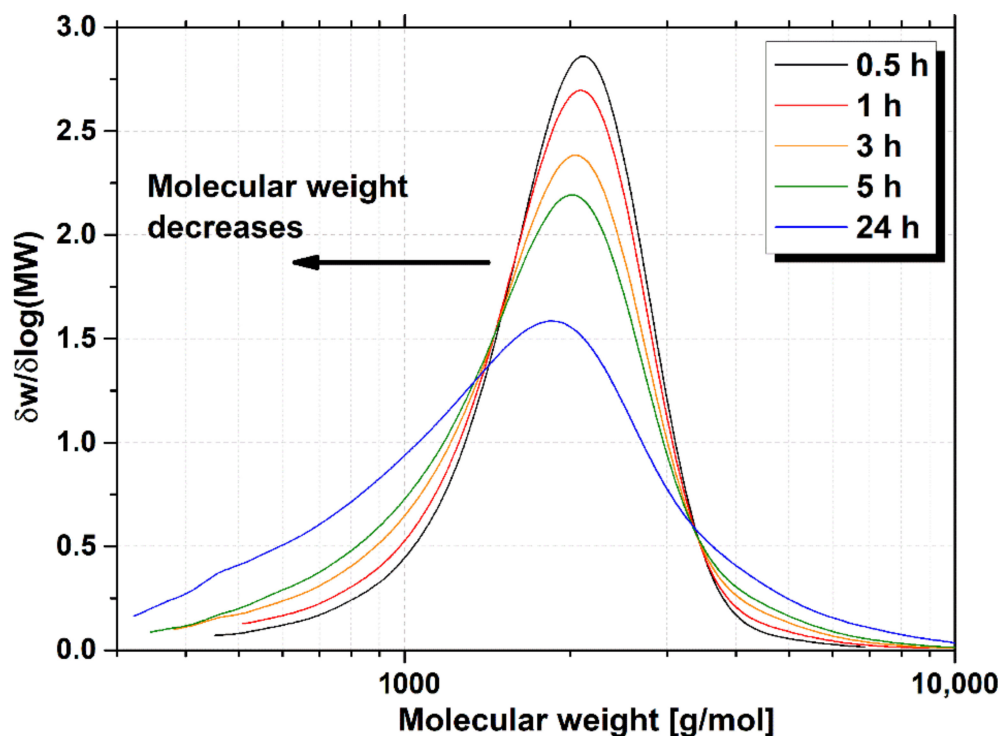


Figure 5. Evolution of the resin molecular weight after heat treatment at 215 °C as a function of time.

To prove that the crosslinking reaction follows a radical mechanism in SBR/poly(α MSt-co-St), a fresh blend was prepared with 30 phr of hydroquinone as antioxidant (SBR/poly(α MSt-co-St)₁₅₀/AO₃₀). Figure 6A,B represent the viscoelastic properties of SBR/poly(α MSt-co-St)₁₅₀/AO₃₀ during the heating and cooling ramps, respectively. The presence of hydroquinone clearly inhibits the crosslinking reaction as G' was not increasing during the heating ramp (Figure 6A, red curve), as opposed to the blend prepared without (Figure 6A, black curve). This behavior indicates that the crosslinking of SBR was effectively inhibited in SBR/poly(α MSt-co-St)₁₅₀/AO₃₀. The conclusion was further confirmed by immersing SBR/poly(α MSt-co-St)₁₅₀/AO₃₀ in toluene, resulting in a complete dissolution, whereas SBR/poly(α MSt-co-St)₁₅₀ was swelling. As hydroquinone prevents SBR/poly(α MSt-co-St) from crosslinking, it confirms that the mechanism is initiated and driven by free radicals, presumably coming from the thermal depolymerization of poly(α MSt-co-St) resin.

Interestingly, the SBR/poly(α MSt-co-St)₁₅₀/AO₃₀ blend still exhibits a clear phase separation of poly(α MSt-co-St) resin, even after the heat treatment at 215 °C. In addition, the resin was extracted from SBR/poly(α MSt-co-St)₁₅₀/AO₃₀ to assess the influence of the antioxidant on the resin depolymerization and revealed a quasi-identical molecular weight distribution. These results indicate that the compatibilization of SBR and poly(α MSt-co-St) is also driven by a radical mechanism and is not only due to a decrease of the resin molecular weight.

This compatibilization could be explained by similar observations performed during the preparation of interpenetrated polymer networks (IPN). IPN are a combination of two polymer networks, where at least one of the two polymers is crosslinked in the immediate presence of the other [46,47]. Several pairs of IPN have been made miscible, for instance by introducing a compatibilizer [48–50]. In such a situation, the addition of a compatibilizer generally aims at promoting the interactions at the interface between the two immiscible phases and to move their surface energies toward each other [51,52]. Among the different ways to compatibilize polymer blends or networks, the co-reaction of the two networks, or the partial grafting of one of the polymers to the second one, is a good way to enhance their chemical affinity, and their compatibility as well [4]. This last assumption stands as the most probable explanation of the compatibilization between SBR and poly(α MSt-co-St).

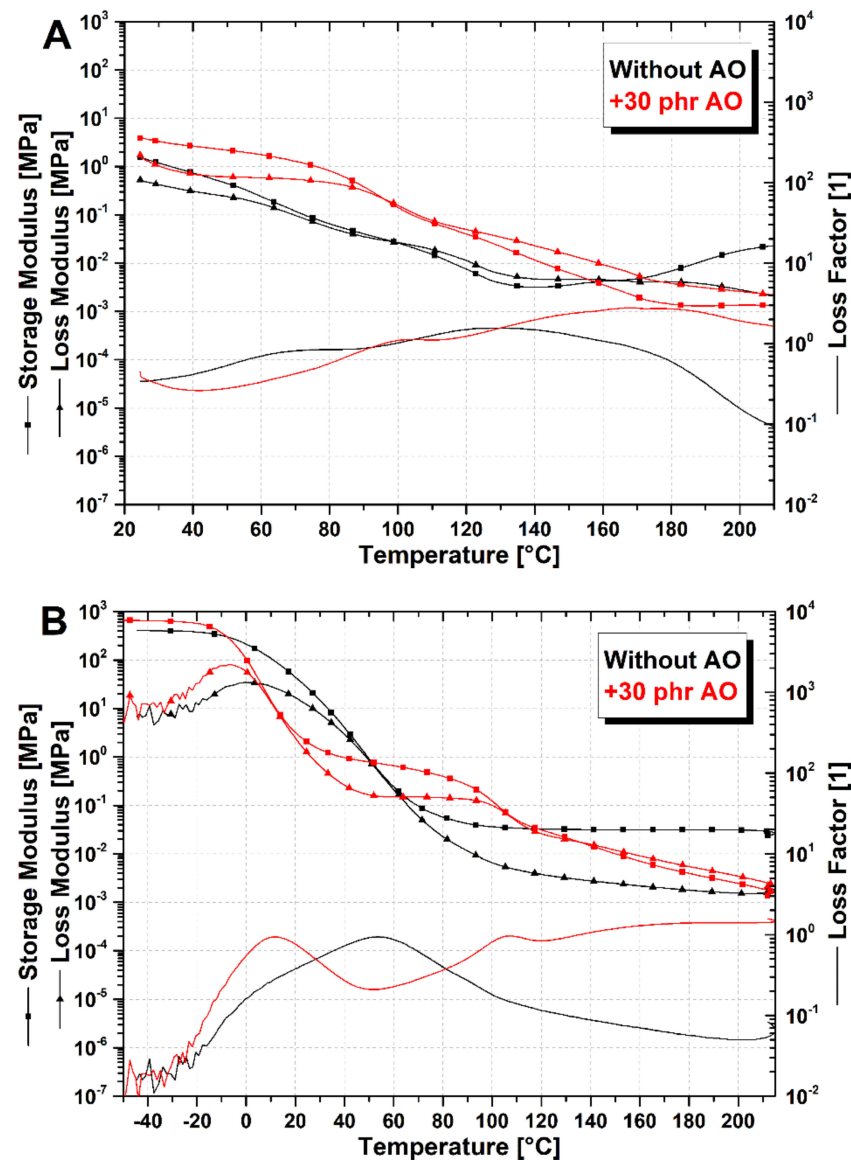


Figure 6. Viscoelastic properties of SBR/poly(α MSt-*co*-St)₁₅₀ (black curves) and SBR/poly(α MSt-*co*-St)₁₅₀/AO₃₀ (red curves) blends during (A) heating up from 20 to 215 °C and (B) cooling down from 215 to −50 °C.

In an attempt to determine if the SBR structural features were modified during its crosslinking in the presence of poly(α MSt-*co*-St), solid-state NMR (ssNMR) was performed after the complete removal of the resin by solvent extraction. The crosslinked-SBR induced by the resin was named CrR-SBR. The same experiment was done on an SBR sample crosslinked by using dicumyl peroxide (DCP). The resulting product was named CrDCP-SBR (see Supplementary Materials, Section S7). Both crosslinked rubbers were compared to the neat SBR (liquid state NMR). Figure 7 shows a zoom of the ¹³C NMR in the aliphatic -CH₂- carbon region of SBR. As depicted on Figure 7, the fingerprint of the aliphatic carbons of SBR was not affected significantly when the rubber was crosslinked with DCP (blue curve). On the other hand, when the rubber was crosslinked in the presence of the poly(α MSt-*co*-St) resin (red curve), a lot of changes were observed in this region. The major changes are highlighted in the black rectangles. These results point out that the poly(α MSt-*co*-St) resin could be involved in other reactions than initiating the rubber crosslinking reaction. Nevertheless, it is rather difficult to confirm that these changes are related to the grafting of poly(α MSt-*co*-St) fragments onto the SBR chains, but still provide evidence that

SBR encountered structural changes which could explain the promoted miscibility between SBR and the poly(α MSt-*co*-St) resin.

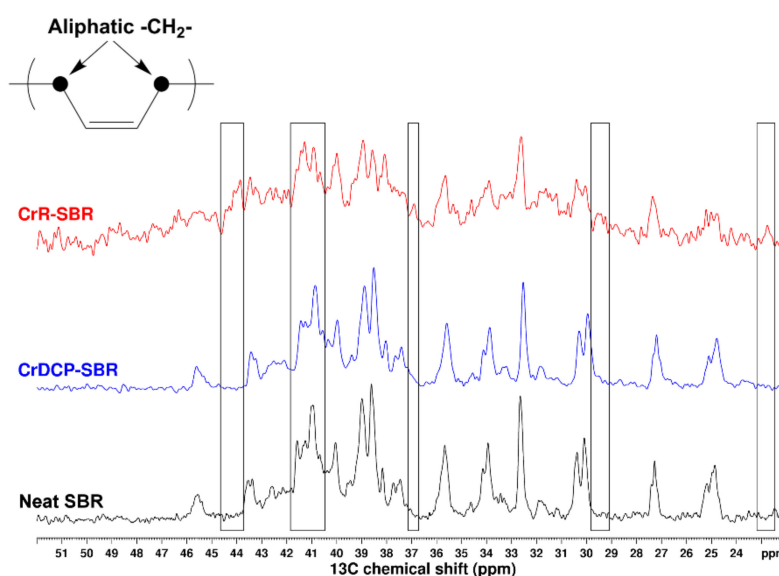


Figure 7. Solid-State ¹³C NMR spectra of CrR-SBR (red curve) and CrDCP-SBR (blue curve). For comparison, the ¹³C liquid NMR spectra of neat SBR is given (black curve).

In the light of all the elements gathered during this study, it can be concluded that the chemical modification encountered by the SBR chains could be the result of a modification due to the species coming from the depolymerization of poly(α MSt-*co*-St). By their reaction with the chains of SBR, they would modify the affinity of the rubber network toward poly(α MSt-*co*-St), improving the miscibility between the resin and SBR. This reaction could be a typical case of reactive compatibilization observed during the synthesis of interpenetrating polymer networks [4]. To further confirm the enhanced affinity of CrR-SBR compared to neat SBR toward poly(α MSt-*co*-St), CrR-SBR was immersed in a solution containing the equivalent of 150 phr of resin solubilized in toluene. Here, the aim was to reintroduce the resin into the network and to analyze its viscoelastic behavior. It was assumed that if the affinity of the rubber network toward poly(α MSt-*co*-St) was enhanced, it would result in a shift of the immiscibility threshold toward higher resin concentration.

The conditions of the experiments were fine-tuned for the crosslinked network CrR-SBR to be able to trap 150 phr of resin. The material after the re-introduction of the resin was renamed CrR-SBR/poly(α MSt-*co*-St)₁₅₀, for the sake of clarity. Figure 8B represents the viscoelastic properties of the material compared to a normal SBR/poly(α MSt-*co*-St)₁₅₀ blend before (blue curves) and after the thermal treatment leading to the enhanced compatibilization of the resin (black curves).

The T_g of CrR-SBR was similar to the neat SBR, indicating a low level of crosslinking density (see Supplementary Materials, Section S8, Figure S6). In CrR-SBR/poly(α MSt-*co*-St)₁₅₀ (Figure 8A, red curves), the incorporation of the resin leads to drastic changes compared to SBR/poly(α MSt-*co*-St)₁₅₀ after treatment at 160 °C (Figure 8A, blue curves). The viscoelastic behavior of CrR-SBR/poly(α MSt-*co*-St)₁₅₀ is closer to the compatibilized case (Figure 8A, black curves), confirming the enhanced compatibility between the two materials [51,52].

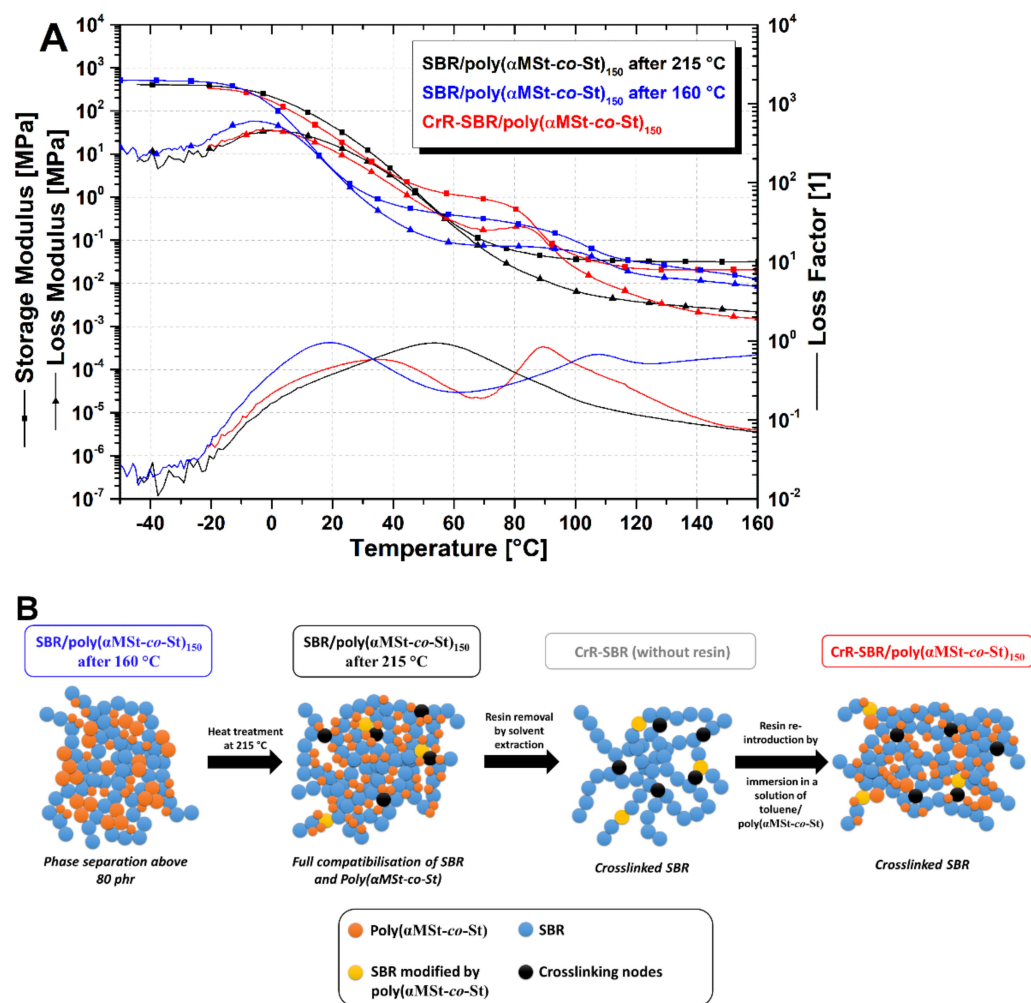


Figure 8. (A) Viscoelastic properties of CrR-SBR/poly(αMSt-co-St)₁₅₀ (red curves) and SBR/poly(MSt-co-St)₁₅₀ before (blue curves) and after the heat treatment at 215 °C (black curves). Measured during cooling ramp (5 °C/min) from 160 to −50 °C. (B) Schematic representation of blend state after each different step.

5. Conclusions

In conclusion, these results demonstrate that the heating of blends of SBR and poly(αMSt-co-St) resins above 215 °C leads to their compatibilization. The reaction follows a radical pathway, resulting from the thermal depolymerization of poly(αMSt-co-St) as demonstrated by GPC measurements. The generated free radicals would trigger the grafting of the resin onto the SBR chains, resulting in an improvement of their compatibility, as attested by the shift of the immiscibility threshold from 80 phr to over 150 phr. To the best of our knowledge, such a thermally induced compatibilization has never been reported despite several decades of fundamental studies and industrial utilization of SBR and poly(αMSt-co-St) resins.

Supplementary Materials: The following are available online at <https://www.mdpi.com/article/10.3390/polym13081267/s1>, Figure S1: Evidence of the irreversibility of resin compatibilization in SBR after the heat treatment at 215 °C. Identical viscoelastic properties are retained after multiple heat-cool-heat measurements, Figure S2: Evidence of the resin/rubber phase separation at 160 °C and after cooling back the sample at 25 °C. Scale bars on the images correspond to 2 μm., Figure S3: Supplemental images taken at each temperature. Evidences of the phase separation in other sample location. Scale bars on the images correspond to 2 μm., Figure S4: Nanomechanical properties of the different samples, Figure S5: Thermal stability of neat SBR up to 225 °C, Figure S6: Comparison of

the viscoelastic behavior of neat SBR versus CrR-SBR, Table S1: Summary of the poly(α MSt-co-St) resins blended in SBR.

Author Contributions: Methodology, A.W.; investigation, A.W.; AFM analysis, J.P.C.F.; NMR analyses, C.Y. and R.D.; validation, P.V., L.P. and M.W.; writing—original draft preparation, A.W.; writing—review and editing, P.V., L.P. and M.W.; supervision, P.V.; project administration, P.V., L.P. and M.W. All authors have read and agreed to the published version of the manuscript.

Funding: This project was supported by the Fonds National de la Recherche under award number IPBG16/11514551/TireMat-Tech.

Institutional Review Board Statement: Not applicable.

Informed Consent Statement: Not applicable.

Data Availability Statement: Data is contained within the article or Supplementary Materials.

Acknowledgments: The authors would like to thank the Luxembourg National Research Fund (FNR) for the funding of the project IPBG TireMat-Tech, SOiA (Grant number: IPBG16/11514551/TireMat-Tech).

Conflicts of Interest: The authors declare no conflict of interest.

Abbreviations

Poly(α MSt-co-St), α -methylstyrene/styrene resin; SBR, styrene-butadiene rubber; T_g , glass transition temperature; phr, part per hundred of rubber; RIPS, reaction-induced phase separation; DCP, dicumyl peroxide; THF, tetrahydrofuran; PTFE, poly(tetrafluoroethylene); AFM, atomic force microscopy, AM-FM, amplitude modulation-frequency modulation; PEEK, poly(ether ether ketone); G' , storage modulus; G'' , loss modulus; σ_{im} , immiscibility threshold; V_e , crosslink density; AO, antioxidant; GPC, gel permeation chromatography; IPN, interpenetrated network; ssNMR, solid-state nuclear magnetic resonance; CrDCP-SBR, styrene-butadiene rubber crosslinked with dicumyl peroxide; CrR-SBR, styrene-butadiene rubber crosslinked with α -methylstyrene/styrene resin.

References

1. Paul, D.; Barlow, J. Polymer blends. *J. Macromol. Sci. Macromol. Chem.* **1980**, *18*, 109–168. [CrossRef]
2. Paul, D.R.; Newman, S. *Polymer Blends*; Academic Press: New York, NY, USA, 1978; Volume 2. Available online: <http://site.ebrary.com/id/10700820> (accessed on 22 April 2020).
3. Painter, P.C.; Coleman, M.M. *Essentials of Polymer Science and Engineering*; DEStech Publications: Lancaster, PA, USA, 2009.
4. Wilkie, C.A. *Polymer Blends Handbook*, 2nd ed.; Springer: Dordrecht, The Netherlands, 2014.
5. Kawahara, S.; Akiyama, S.; Kano, Y. Miscibility and pressure-sensitive adhesive properties of poly (vinylethylene-co-1,4-butadiene)/terpene resin blends. *Polymer* **1991**, *32*, 1681–1687. [CrossRef]
6. Fujita, M.; Kajiyama, M.; Takemura, A.; Ono, H.; Mizumachi, H.; Hayashi, S. Effects of miscibility on probe tack of natural-rubber-based pressure-sensitive adhesives. *J. Appl. Polym. Sci.* **1998**, *70*, 771–776. [CrossRef]
7. Vleugels, N.; Pille-Wolf, W.; Dierkes, W.K.; Noordermeer, J.W.M. Understanding the Influence of Oligomeric Resins on Traction and Rolling Resistance of Silica-Reinforced Tire Treads. *Rubber Chem. Technol.* **2015**, *88*, 65–79. [CrossRef]
8. Barlow, F.W. *Rubber Compounding: Principles, Materials, and Techniques*; Dekker, M., Ed.; EBSCO Information Services: New York, NY, USA, 1993. Available online: <http://search.ebscohost.com/login.aspx?direct=true&scope=site&db=nlebk&db=nlabk&AN=47068> (accessed on 21 April 2020).
9. Rodgers, B. *Rubber Compounding: Chemistry and Applications*; CRC Press: Boca Raton, FL, USA, 2016.
10. Rodgers, B.; Waddell, W. Tire engineering. In *The Science and Technology of Rubber*; Elsevier: Amsterdam, The Netherlands, 2013; pp. 653–695. Available online: <http://linkinghub.elsevier.com/retrieve/pii/B9780123945846000145> (accessed on 16 October 2017).
11. Heinrich, G.; Vilgis, T. Why silica technology needs S-SBR in high performance tires? *Kautsch. Gummi Kunstst.* **2008**, *61*, 368–376.
12. Hays, D.; Browne, A.L. *The Physics of Tire Traction: Theory and Experiment*; Springer: New York, NY, USA, 2013. Available online: <https://public.ebookcentral.proquest.com/choice/publicfullrecord.aspx?p=5575702> (accessed on 9 April 2020).
13. Kim, S.W.; Lee, G.H.; Heo, G.S. Identification of Tackifying Resins and Reinforcing Resins in Cured Rubber. *Rubber Chem. Technol.* **1999**, *72*, 181–198. [CrossRef]
14. Powers, P.O. Resins Used in Rubber. *Rubber Chem. Technol.* **1963**, *36*, 1542–1570. [CrossRef]
15. Class, J.B.; Chu, S.G. The viscoelastic properties of rubber–resin blends. I. The effect of resin structure. *J. Appl. Polym. Sci.* **1985**, *30*, 805–814. [CrossRef]

16. Class, J.B.; Chu, S.G. The viscoelastic properties of rubber–resin blends. II. The effect of resin molecular weight. *J. Appl. Polym. Sci.* **1985**, *30*, 815–824. [[CrossRef](#)]
17. Class, J.B.; Chu, S.G. The viscoelastic properties of rubber–resin blends. III. The effect of resin concentration. *J. Appl. Polym. Sci.* **1985**, *30*, 825–842. [[CrossRef](#)]
18. Akiyama, S. Phase behavior and pressure sensitive adhesive properties in blends of poly (styrene-*b*-isoprene-*b*-styrene) with tackifier resin. *Polymer* **2000**, *41*, 4021–4027. [[CrossRef](#)]
19. Aubrey, D.W.; Sherriff, M. Viscoelasticity of rubber-resin mixtures. *J. Polym. Sci. Polym. Chem. Ed.* **1978**, *16*, 2631–2643. [[CrossRef](#)]
20. Aubrey, D.W.; Sherriff, M. Peel adhesion and viscoelasticity of rubber–resin blends. *J. Polym. Sci. Polym. Chem. Ed.* **1980**, *18*, 2597–2608. [[CrossRef](#)]
21. Copley, B.C. Tackification Studies of Natural Rubber/Styrene-Butadiene Rubber Blends. *Rubber Chem. Technol.* **1982**, *55*, 416–427. [[CrossRef](#)]
22. L’Heveder, S.; Sportelli, F.; Isitman, N.A. Investigation of solubility in plasticised rubber systems for tire applications. *Plast. Rubber Compos.* **2016**, *45*, 1–7. [[CrossRef](#)]
23. Flory, P.J. *Principles of Polymer Chemistry*, 3rd ed.; Springer: New York, NY, USA, 1953.
24. Rubinstein, M.; Colby, R.H. *Polymer Physics*; Oxford University Press: Oxford, UK; New York, NY, USA, 2003.
25. Teraoka, I. *Polymer solutions: An introduction to Physical Properties*; Wiley: New York, NY, USA, 2002.
26. Wolf, A.; Desport, J.S.; Dieden, R.; Frache, G.; Weydert, M.; Poorters, L.; Schmidt, D.F.; Verge, P. Sequence-Controlled α -Methylstyrene/Styrene Copolymers: Syntheses and Sequence Distribution Resolution. *Macromolecules* **2020**, *53*, 8032–8040. [[CrossRef](#)]
27. Chen, W.; Kobayashi, S.; Inoue, T.; Ohnaga, T.; Ougizawa, T. Polymerization-induced spinodal decomposition of poly(ethylene-co-vinyl acetate)methyl methacrylate mixture and the influence of incorporating poly(vinyl acetate) macromonomer. *Polymer* **1994**, *35*, 4015–4021. [[CrossRef](#)]
28. Yamanaka, K.; Takagi, Y.; Inoue, T. Reaction-induced phase separation in rubber-modified epoxy resins. *Polymer* **1989**, *30*, 1839–1844. [[CrossRef](#)]
29. Yamanaka, K.; Inoue, T. Phase separation mechanism of rubber-modified epoxy. *J. Mater. Sci.* **1990**, *25*, 241–245. [[CrossRef](#)]
30. Yamanaka, K.; Inoue, T. Structure development in epoxy resin modified with poly(ether sulphone). *Polymer* **1989**, *30*, 662–667. [[CrossRef](#)]
31. Visconti, S.; Marchessault, R.H. Small Angle Light Scattering by Elastomer-Reinforced Epoxy Resins. *Macromolecules* **1974**, *7*, 913–917. [[CrossRef](#)]
32. Okada, M.; Fujimoto, K.; Nose, T. Phase Separation Induced by Polymerization of 2-Chlorostyrene in a Polystyrene/Dibutyl Phthalate Mixture. *Macromolecules* **1995**, *28*, 1795–1800. [[CrossRef](#)]
33. Kojima, T.; Ohnaga, T.; Inoue, T. Two-phases structure and mechanical properties of poly(methyl methacrylate)/poly(ethylene-co-vinylacetate) alloys by polymerization-induced phase decomposition. *Polymer* **1995**, *36*, 2197–2201. [[CrossRef](#)]
34. Manzione, L.T.; Gillham, J.K.; McPherson, C.A. Rubber-modified epoxies. I. Transitions and morphology. *J. Appl. Polym. Sci.* **1981**, *26*, 889–905. [[CrossRef](#)]
35. Williams, M.L.; Landel, R.F.; Ferry, J.D. The Temperature Dependence of Relaxation Mechanisms in Amorphous Polymers and Other Glass-forming Liquids. *J. Am. Chem. Soc.* **1955**, *77*, 3701–3707. [[CrossRef](#)]
36. Ferry, J.D. *Viscoelastic Properties of Polymers*, 3rd ed.; Wiley: New York, NY, USA, 1980.
37. Mark, J.E. (Ed.) *Polymer Data Handbook*; Oxford University Press: New York, NY, USA, 1999.
38. Bamford, C.H.; Tipper, C.F.H. *Degradation of Polymers*; Elsevier Scientific Publishing Co: Amsterdam, The Netherlands; New York, NY, USA, 1975.
39. Guaita, M.; Chiantore, O. Molecular mass changes in the thermal degradation of poly- α -methylstyrene. *Polym. Degrad. Stab.* **1985**, *11*, 167–179. [[CrossRef](#)]
40. Murakata, T.; Saito, Y.; Yosikawa, T.; Suzuki, T.; Sato, S. Solvent effect on thermal degradation of polystyrene and poly- α -methylstyrene. *Polymer* **1993**, *34*, 1436–1439. [[CrossRef](#)]
41. Kruželák, J.; Sýkora, R.; Hudec, I. Vulcanization of Rubber Compounds with Peroxide Curing Systems. *Rubber Chem. Technol.* **2017**, *90*, 60–88. [[CrossRef](#)]
42. Liu, X.; Zhou, T.; Liu, Y.; Zhang, A.; Yuan, C.; Zhang, W. Cross-linking process of cis-polybutadiene rubber with peroxides studied by two-dimensional infrared correlation spectroscopy: A detailed tracking. *RSC Adv.* **2015**, *5*, 10231–10242. [[CrossRef](#)]
43. Sasuga, T.; Takehisa, M. Effect of high pressure on radiation-induced cross-linking of synthetic rubbers. *J. Macromol. Sci. Part B* **1975**, *11*, 389–401. [[CrossRef](#)]
44. Xing, W.; Li, H.; Huang, G.; Cai, L.-H.; Wu, J. Graphene oxide induced crosslinking and reinforcement of elastomers. *Compos. Sci. Technol.* **2017**, *144*, 223–229. [[CrossRef](#)]
45. Valentin, J.L.; Rodriguez, A.; Marcos-Fernandez, A.; González, L. Dicumyl peroxide cross-linking of nitrile rubbers with different content in acrylonitrile. *J. Appl. Polym. Sci.* **2005**, *96*, 1–5. [[CrossRef](#)]
46. Sperling, L.H. Interpenetrating polymer networks: An overview. In *Interpenetrating Polymer Networks*; Klemperer, D., Sperling, L.H., Utracki, L.A., Eds.; American Chemical Society: Washington, DC, USA, 1994; pp. 3–38. [[CrossRef](#)]
47. Sperling, L.H. *Interpenetrating Polymer Networks and Related Materials*, 1st ed.; Springer: Berlin/Heidelberg, Germany, 1981.

48. Kim, S.C.; Sperling, L.H. (Eds.) *IPNs around the World: Science and Engineering*; John Wiley: Chichester, UK; New York, NY, USA, 1997.
49. Wu, X.; He, G.; Yan, X.; Li, X.; Xiao, W.; Jiang, X. Miscibility, morphology, and phase behavior of IPNs. In *Micro- and Nano-Structured Interpenetrating Polymer Networks*; Thomas, S., Grande, D., Cvelbar, U., Raju, K.V.S.N., Narayan, R., Thomas, S.P., Akhina, H., Eds.; John Wiley & Sons, Inc.: Hoboken, NJ, USA, 2016; pp. 29–68. [[CrossRef](#)]
50. Lipatov, I.S.; Alekseeva, T. *Phase-Separated Interpenetrating Polymer Networks*; Springer: Berlin, Germany; New York, NY, USA, 2007.
51. Rigoussen, A.; Verge, P.; Raquez, J.-M.; Dubois, P. Natural Phenolic Antioxidants As a Source of Biocompatibilizers for Immiscible Polymer Blends. *ACS Sustain. Chem. Eng.* **2018**, *6*, 13349–13357. [[CrossRef](#)]
52. Rigoussen, A.; Verge, P.; Raquez, J.-M.; Habibi, Y.; Dubois, P. In-depth investigation on the effect and role of cardanol in the compatibilization of PLA/ABS immiscible blends by reactive extrusion. *Eur. Polym. J.* **2017**, *93*, 272–283. [[CrossRef](#)]